Theor Chem Acc (1997) 97:277–282

Theoretical
Chemistry Accounts

Formation of 2-hexene by cationic dimerization of propene: an ab initio and density functional theory study

N. Salhi-Benachenhou[1], J. R. Alvarez-Idaboy[1,*], S. Lunell[1], L. A. Eriksson[2]

[1] Department of Quantum Chemistry, Uppsala University, P.O. Box 518, S-751 20 Uppsala, Sweden
[2] Department of Physics, Stockholm University, P.O. Box 6730, S-113 85 Stockholm, Sweden

Received: 17 December 1996 / Accepted: 12 May 1997

Abstract. The formation of a 2-hexene radical cation from a propene radical cation and a neutral propene molecule is investigated by means of ab initio UHF and spin projected MP2 calculations, as well as the SVWN and B3LYP levels of density functional theory. A stable addition complex, with loose CC bonds, is found. To proceed from the addition complex to the product, a locally planar transition state must be passed, with a migrating hydrogen located half-way between the donating and the accepting carbon atoms. At the highest computational levels considered, PMP2/6-31G(*d*,*p*)//MP2/3-21G and B3LYP/6-31G(*d*,*p*), this transition state lies approximately 11 and 13 kcal/mol, respectively, above the addition complex. The high barrier is believed to be one reason why radical cation oligomerization of propene has not been detected experimentally, in contrast to the case of ethene, where the corresponding barrier is only a few kcal/mol.

Key words: Propene cation – Cationic dimerization – 2-Hexene

1 Introduction

Radical cations of olefins occur as important intermediates in catalytic reactions and cationic polymerizations, and also as short-lived species with a natural tendency towards decomposition [1]. As a consequence, they are difficult to study experimentally. On the theoretical side, one complication resides in the fact that even though the neutral molecule may be planar, the cationic moieties often have a local non-planarity introduced about the ionized π-bond. Contradictory conclusions concerning the value of the torsion angles are in some cases given by different authors. In turn, inconclusive assignments are deduced for the ESR spectra, which are known to be very sensitive to the geometry. For instance, while similar structures of the ethene radical cation have been obtained in vacuum ultraviolet and photoelectron experiments [2], several values of the twist angle around the double bond have been proposed in various theoretical investigations [3]. Moreover, the ESR determination of the structure of the ethene cation is hampered by its strong tendency to form dimers and higher oligomers [4].

Recently, the ethene-ethene radical cation addition reaction was investigated [5] by means of ab initio UHF, MP2 and MP4 methods using 3-21G, 6-31G and 6-31G(*d*,*p*) basis sets. A mechanism for the reaction was suggested where an intermediate addition complex and a transition state were identified. The final product was the 1-butene radical cation. It was found that the formation of the addition complex proceeds without activation energy, and that the activation energy for the rearrangement to a 1-butene radical cation is very low [5]. These facts were interpreted by the authors as being a possible justification for the observed reactions [4b]. The ethene-ethene radical cation addition reaction has been independently investigated by a second group of authors, using the UHF, UMP2 and QCISD(T) methods and a 6-31G(*d*) basis set [6]. In the two parallel studies, essentially the same conclusions were derived with regard to structures and reaction paths. The formation of the 1-butene radical cation in the above mentioned ESR experiments [4b] was also interpreted in the latter paper as being a two-step addition reaction of the ethene radical cation with its neutral parent molecule, supporting the theoretical mechanism found in Ref. [5]. The trimerization reaction, being the next step in the radical cation oligomerization of ethene by addition of a second neutral ethene molecule to the 1-butene radical cation and yielding the 1-hexene radical cation, has also been theoretically investigated. [7].

No such reactions have yet been observed for the radical cation of propene, though some results have been reported [8] regarding the geometry description and ESR analysis. Because of the structural analogies between

Permanent address: Facultad de Quimica, Universidad de la Habana, 10400, Cuba

Correspondence to: S. Lunell

ethene and propene radical cations, one could suspect that the latter should show the same type of oligomerization reactions as the former. Experimental results, however, suggest that the propene cation is less reactive than the ethene radical cation, since it has been possible to observe the former in a frozen halocarbon matrix at 77 K [8b] while, at this temperature, the latter is reported to react [4b]. On the other hand, the radical cation of isobutene, which is a methyl substituted propene, is reported to undergo reactions similar to those of ethene [9]. From the structural point of view, it therefore seems reasonable to expect that a reaction which is common to ethene and isobutene radical cations should also be possible for the propene radical cation.

In the present paper, we study theoretically the addition reaction between a propene radical cation and a neutral propene molecule. Because of the asymmetry of the propene molecule, several topologically inequivalent addition reactions can be imagined, in contrast to the one possible reaction for ethene. These different alternatives are discussed in the first paragraphs of Sect. 3, while the bulk of the discussion is devoted to the specific reaction giving 2-hexene as its final product.

2 Method

In order to obtain an energy profile for the processes studied, a search was made for local minima and stationary points. A full optimization of the geometry was first performed at the ab initio UHF [10] level in conjunction with the 3-21G basis set [11]. Since correlation effects were found to be important in previous studies [5–7], the structures of the stationary points obtained at the UHF/3-21G level were also optimized using Møller-Plesset perturbation theory [12] to the second order (MP2). Because of the well-known hazards of performing MP2 calculations with such a small basis set [13], the latter was extended in a third step and augmented by polarization functions, to give the 6-31G(*d*,*p*) basis set [14]. With this basis set, single-point spin projected MP2 (PMP2) calculations were performed (PMP2/6-31G(*d*,*p*)//MP2/3-21G) to allow for the removal of spin contamination. In addition, the geometries of the stationary points were fully optimized at different levels of density functional theory (DFT): SVWN/3-21G, B3LYP/3-21G and B3LYP/6-31G(*d*,*p*). Slater's exchange term [15] and, for the correlation term, the Vosko, Wilks and Nusair parametrization [16] were used in the SVWN (LDA) functional. The gradient corrected (non-local) B3LYP functional uses the three-parameter hybrid exchange of Becke (B3) [17], together with the correlation correction of Lee, Yang and Parr (LYP) [18].

All the ab initio and DFT energies were corrected for the basis set superposition error (BSSE) using the counterpoise procedure of Boys and Bernardi [19]. Since the quantitative reliability of this procedure has been questioned in some instances [20, 21], especially at correlated levels [22], the magnitude of the counterpoise corrections is shown separately in the tables, to facilitate comparison with other work. In our previous papers [5, 7] it was mistakenly stated that the BSSE was negligible at the MP2/6-31G(*d*,*p*) level. The importance of BSSE in this case was clearly demonstrated by Jungwirth and Bally [6]. All the ab initio energies reported in the present paper are hence corrected for the BSSE. A frequency calculation at the UHF/3-21G level was performed to obtain the zero-point vibrational energy contribution (ZPE). The energies at the highest ab initio level, PMP2/6-31G(*d*,*p*) were corrected with the ZPE calculated at the Hartree-Fock level, a procedure which has been found to be satisfactory in previous investigations [21].

All the post-SCF calculations were performed within the frozen-core approximation. The GAUSSIAN 92[23] and GAUSSIAN 94 [24] program packages were used for all the ab initio and DFT calculations.

3 Results and discussion

All the structures involved at the various steps of the propene–propene radical cation addition reaction were optimized, without any symmetry constraints, at the UHF/3-21G, MP2/3-21G, SVWN/3-21G, B3LYP/3-21G and B3LYP/6-31G(*d*,*p*) levels. First, the way the two molecules approach each other was studied. In Fig. 1, the two propene moieties are represented and the labels used in the following geometry description are indicated.

In contrast to the analogous reaction with ethene, where there is only one possible way to connect the two molecules, three different connection schemes are possible in the propene case, namely a tail-to-tail (C3-C4), a head-to-tail (C2-C4) and a head-to-head (C2-C5) connection (cf. Fig. 1).

Comparing the stability of the three addition complexes, the head-to-head complex is obviously expected to be much less stable than the other two complexes because of steric effects. This expectation was confirmed by the results of semiempirical PM3 calculations, which placed the head-to-head complex 23 kcal/mol higher in energy than the tail-to-tail complex. Moreover, the MP2/3-21G optimization calculations on the head-to-head complex led to a non-bonding situation. Finally, with the B3LYP/6-31G(*d*,*p*) method, a starting head-to-head geometry optimized to the tail-to-tail complex. The head-to-head reaction path will therefore not be discussed further.

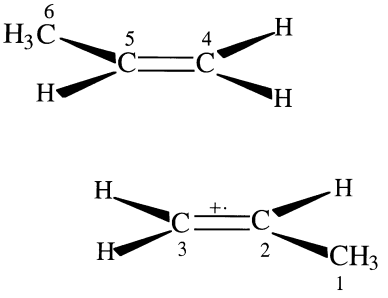

Fig. 1. Labelling of the carbon atoms of the propene + propene radical cation supermolecule

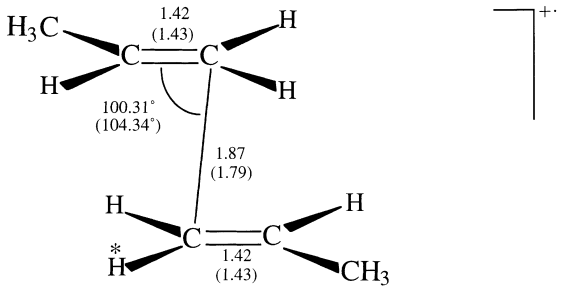

Fig. 2. Optimized geometries of the tail-to-tail addition complex at the MP2/3-21G (B3LYP/6-31G(*d,p*)) levels. The migrating hydrogen is denoted by an *asterisk*

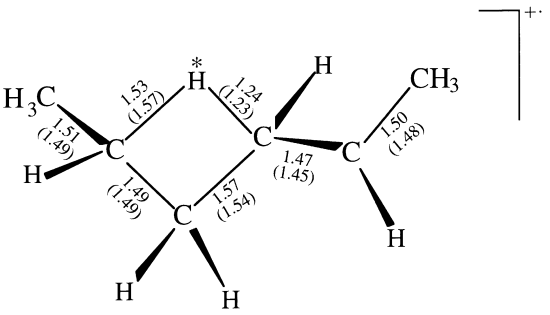

Fig. 3. Optimized geometries of the transition state of the tail-to-tail addition reaction at the MP2/3-21G (B3LYP/6-31G(*d,p*)) levels

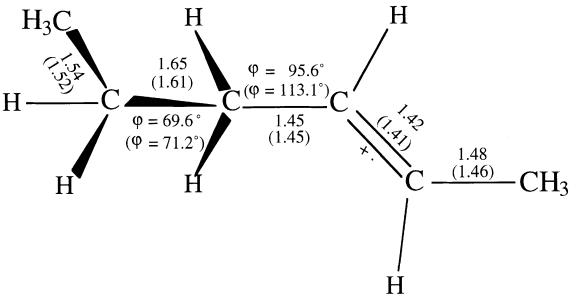

Fig. 4. Optimized geometries of the final product of the tail-to-tail addition reaction at the MP2/3-21G (B3LYP/6-31G(*d,p*)) levels

The head-to-tail addition complex was calculated by the MP2/3-21G method to lie 4.6 kcal/mol higher in energy than the tail-to-tail complex. Head-to-tail addition would be the first step in the formation of 4-methyl-2-pentene rather than 2-hexene. In a complete study, this reaction channel should also be considered. In the present paper, however, we limit ourselves to the tail-to-tail addition reaction and subsequent steps. It should be noted that in the related case of isobutene, the tail-to-tail connection is the only one observed experimentally [25] as well as theoretically [26]. With the B3LYP/6-31G(*d,p*) method, a starting head-to-tail geometry optimized to the tail-to-tail complex.

The main data of the MP2/3-21G and B3LYP/6-31G(*d,p*) geometry optimization calculations on the tail-to-tail addition complex are displayed in Fig. 2. Benefiting from the experience of the previous study with ethene, a starting geometry of 2.09 Å and 180° for the bond length and the torsion angle between the two moieties, respectively, was optimized. After the optimization, both methods predict a loose complex with appreciably weakened bonds and a symmetric structure around the elongated single bond.

The next step in the addition reaction involves hydrogen migration either from C3 to C5 or from C4 to C2, both processes being symmetrically equivalent and leading to the same final product, the 2-hexene radical cation. To search for a possible transition state, the same procedure was used as for the corresponding reaction involving ethene [5]. The C5-H* distance was decreased stepwise from the value it had in the addition complex, using the reaction coordinate method implemented in the semiempirical MOPAC program [27]. The point with maximum heat of formation and minimum gradient was optimized to a transition state structure, first at the semiempirical level and then with the UHF/3-21G, MP2/3-21G, SVWN/3-21G, B3LYP/3-21G and B3LYP/6-31G(*d,p*) methods, and characterized at the UHF/3-21G level by one imaginary frequency of magnitude 878 cm^{-1}.

The MP2/3-21G and the B3LYP/6-31G(*d,p*) optimized geometries of the transition state are shown in Fig. 3. A locally planar four-membered ring structure was found where the migrating hydrogen atom is located between the donating and accepting carbon atoms. One notes that both methods generally predict very similar geometries.

The final product of the propene–propene radical cation addition reaction, the trans-2-hexene radical cation, is displayed in Fig. 4. Similarly in the final product of the cationic trimerization of ethene [7], i.e the 1-hexene radical cation, a non-planar structure is predicted for the 2-hexene cation. The torsion angle around the double bond has, however, negligible values ranging from 0.5° (MP2/3-21G) to 3.5° (B3LYP/6-31G(*d,p*)), and can therefore be considered as representing a locally planar structure. Twisting is otherwise found around the CC single bonds, as depicted in the figure. The results of the geometry optimizations with the MP2/3-21G, UHF/3-21G and B3LYP/6-31G(*d,p*) methods point to a gauche structure around the C4-C5 bond with a torsion angle of 69°, on the average, while the torsion angle around the C3-C4 bond optimizes to 95.6°, 108.3° and 113.1° in the MP2, UHF and B3LYP calculations, respectively. Concerning the calculated bond lengths, the only significant spread is observed for the C4-C5 bond, which is found to be 1.65 Å, 1.58 Å and 1.61 Å at the MP2, UHF and B3LYP levels, respectively.

The unpaired spin density in the addition complex is mainly located on the carbon atoms C2 and C5, both of which show a Mulliken spin density of 0.525 in the MP2/6-31G(*d,p*) calculation. With such a spin distribution, the addition complex can be regarded as a delocalized 2,4-diyl radical cation, similar to the cyclohexane-1,4-diyl radical cation for which the ESR evidence was given by Williams et al. [28].

In Table 1 we have collected the energy differences between the free reactants and, successively, the addition complex, the transition state and the final product of the tail-to-tail addition reaction, obtained at the various

Table 1. Relative energies (in kcal/mol) of the species entering the propene + propene radical cation reaction in the tail-to-tail connection scheme, with respect to the isolated reactants, as obtained at different levels of calculation. All the energies are corrected for basis set superposition error (BSSE). As an indication of its order of magnitude, the counterpoise correction (CP) for the addition complex is given in parentheses

Level of calculation	Relative energies			CP
	Addition complex	Transition state	Product	
UHF/3-21G	−16.6	+3.6	−30.3	(7.4)
MP2/3-21G	−18.9	−1.8	−30.3	(12.2)
PMP2/3-21G//MP2/3-21G	−23.5	−2.9	−30.4	(12.3)
MP2/6-31G(*d,p*)//MP2/3-21G	−24.3	−17.1	−39.3	(5.5)
PMP2/6-31G(*d,p*)//MP2/3-21G	−29.4	−18.2	−39.4	(5.5)
– ″ –, including ZPE[a]	−26.3	−16.9	−35.3	(5.5)
SVWN/3-21G	−49.3	−38.7	−58.11	(7.7)
B3LYP/3-21G	−33.2	−14.9	−42.3	(4.3)
B3LYP/6-31G(*d,p*)	−30.5	−17.5	−41.9	(1.6)

[a] Calculated at the UHF/3-21G level

Table 2. Absolute energies (in atomic units) of the stationary points on the potential energy surface of the propene + propene radical cation reaction in the tail-to-tail connection scheme, obtained at the UHF/3-21G, PMP2/3-21G//MP2/3-21G and PMP2/6-31G(*d,p*)//MP2/3-21G levels of calculation, plus the zero-point vibrational energy contributions (ZPE) as computed with UHF/3-21G

	UHF/3-21G	PMP2/3-21G	PMP2/6-31G(*d,p*)	ZPE
Neutral propene	−116.42401	−116.69485	−117.50344	0.0858
Propene radical cation	−116.11708	−116.35325	−117.15857	0.0828
Neutral propene[a]	−116.43008	−116.70553	−117.50911	0.0858
Propene radical cation[a]	−116.12287	−116.36211	−117.16162	0.0828
Addition complex	−232.57941	−233.10509	−234.71752	0.1736
Transition state	−232.54716	−233.07230	−234.69970	0.1707
Final product	−232.60123	−233.11601	−234.73351	0.1752

[a] Including ghost atoms

ab initio and DFT levels, as indicated. As already mentioned in Sect. 2, all the relative energies have been corrected for the BSSE, while the ZPE, calculated at the UHF/3-21G level, is only added to the final PMP2/6-31G(*d,p*) energies. As an indication of the orders of magnitude of the counterpoise corrections of the addition complex, these are also given in Table 1. The ZPE corrections are reported in Table 2, together with the UHF/3-21G, PMP2/3-21G and PMP2/6-31G(*d,p*) absolute energies. In Fig. 5, the energy profiles are drawn for the single-point PMP2/6-31G(*d,p*)//MP2/3-21G calculations and for the full geometry optimization computation at the DFT levels (SVWN/3-21G, B3LYP/3-21G and B3LYP/6-31G(*d,p*)), as derived from Table 1.

From an examination of Table 1 one can see that, when using the 3-21G basis set, the UHF and MP2 relative energies are found to be very similar for the addition complex. This clearly indicates that the correlation correction is practically the same for the addition complex – where the two propene moieties are connected by a loose bond – and for the free reactants. In turn, because the number of bonds is the same in the reactants and in the product, these have roughly the same correlation correction which also results in similar UHF/3-21G and MP2/3-21G relative energies for the product.

More stable stationary points are generally found at the highest correlated ab initio level, PMP2/6-31G(*d,p*), compared to those obtained with UHF/3-21G and MP2/3-21G. Moreover, the PMP2/6-31G(*d,p*) relative energies were corrected for the ZPE, as reported in the last line of Table 1 (for the ZPE of the different stationary points, see also Table 2). The total ZPE plus BSSE corrections amount to 8.6 kcal/mol and 9.6 kcal/mol for the addition complex and the final product, respectively.

Among the DFT results, the SVWN/3-21G energies are found to be too low. The notorious problem of the overbinding [29] of the LDA functional is hence well reflected here. The relative energies obtained from the gradient-corrected DFT calculations are predicted to lie

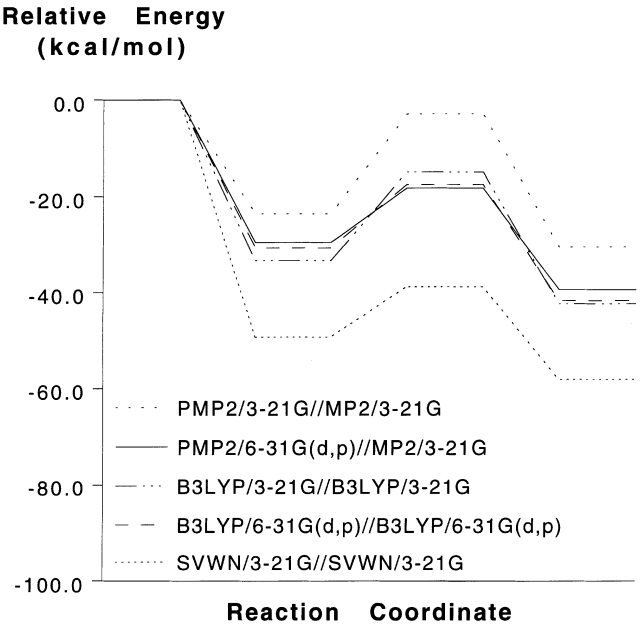

Fig. 5. Relative energies of the addition complex, the transition state and the reaction product of the propene + propene radical cation reaction in the tail-to-tail connection scheme, calculated at the PMP2/3-21G, PMP2/6-31G(*d,p*)//MP2/3-21G, SVWN/3-21G, B3LYP/3-21G, and B3LYP/6-31G(*d,p*) levels of theory. As a reference level, the combined energies of the free reactants are used

very close to those obtained at the highest ab initio level employed here, PMP2/6-31G(*d*,*p*), both when the 3-21G and the 6-31G(*d*,*p*) basis sets were used in the B3LYP method.

These facts are also reflected in Fig. 5. The PMP2/6-31(*d*,*p*), B3LYP/3-21G and the B3LYP/6-31G(*d*,*p*) energy profiles are essentially the same, while the profile obtained at the PMP2/3-21G level is too high, obviously due to the deficiency of the 3-21G basis set, and the SVWN/3-21G profile is too low, due to the overbinding of LDA, as mentioned above.

Also, one notes from Fig. 5 that all the stationary points have a lower energy than the reactants, and that the total heat of reaction is strongly negative (see also, the relative energies for the products in Table 1). In a low-temperature matrix-isolation experiment the possibility cannot be excluded that some or all of the energy released in the first reaction step is absorbed by the surrounding matrix. In such a case, the addition complex may possibly be observed experimentally, lying ca 30 kcal/mol lower than the reactants and ca 12 kcal/mol lower than the transition state, as calculated at highest levels with PMP2/6-31G(*d*,*p*) and B3LYP/6-31G(*d*,*p*).

This reasoning thus follows qualitatively the same line as for ethene [5]. Quantitatively, however the PMP2/6-31G(*d*,*p*)//MP2/6-31G(*d*,*p*) results for ethene predict a much smaller energy difference between the addition complex and the transition state: 4.3 kcal/mol, which increases slightly, to 6.1 kcal/mol, at the PMP4/6-31G(*d*,*p*)//MP2/6-31G(*d*,*p*) level. The final product was furthermore found to be somewhat more stable (−48.9 kcal/mol) with respect to the free reactants, which should be compared with the present BSSE-uncorrected value of −44.9 kcal/mol. This suggests that propene should be expected to be less reactive towards its radical cation than ethene. A second factor affecting the observed rate of the ethene + ethene radical cation reaction is, of course, their higher mobility in the matrix, relative to that of the larger propene molecules.

4 Conclusion

The propene-propene radical cation addition reaction to 2-hexene was investigated using ab initio UHF and MP2 methods as well as at the SVWN and B3LYP levels of DFT. As also observed for the equivalent reactions with ethene, the two reactants initially form a stable addition complex. A transition state is then passed, in which a hydrogen is partially transferred between two carbon atoms, yielding a locally planar square-shaped transition-state structure. The energy difference between the addition complex and the transition state is approximately 12 kcal/mol, as computed in the BSSE corrected PMP2/6-31G(*d*,*p*)//MP2/3-21G and B3LYP/6-31G(*d*,*p*)//B3LYP/6-31G(*d*,*p*) calculations. At the same levels of calculation, the final products lie 11 kcal/mol below the addition complex.

Compared with previous studies on ethene oligomerization, the barriers towards hydrogen migration in the present reaction sequences are found to be much higher: the value obtained in our previous paper at a similar level of accuracy (PMP2/6-31G(*d*,*p*)) was 4.3 kcal/mol for the addition of ethene to the ethene cation [5], while values of 5.9 kcal/mol with QCISD(T)//6-31G(*d*)//MP2/6-31G(*d*) and only 0.7 kcal/mol at the UMP2/6-31G(*d*) level are reported by Jungwirth and Bally [6]. Consequently, whereas the ethene cation was already found to react with neutral ethene molecules at 77 K, no such reaction is observed for propene. Assuming this to be the main reason for the differences in behaviour between the two systems, one may thus expect the propene oligomerization to occur at higher temperatures. A number of other explanations are also possible for the experimentally observed difference in behaviour. The propene radical cation is far more "bulky", and thus its diffusion through the matrix is hindered more, whereas in the case of the ethene cation, the diffusion in the softened matrix was found to be an important factor in the continued reaction [4b].

In the present paper we have not discussed the role of the surrounding matrix in any detail. It was implicitly assumed that all or most of the energy released in the first addition step is absorbed by the matrix, so that the important parameter affecting the reaction probability is the barrier to internal proton rearrangement. The situation would be quite different in gas phase, where the outcome of the reaction would depend on the potential energy surface in a more complex way. The importance of the matrix becomes very clear when studying the competing reaction of deprotonation to an allyl radical, which has been found to be strongly matrix dependent [8b, 9, 30]. Awaiting gas phase experiments, further theoretical work, incorporating the effect of the surrounding matrix explicitly, would be needed for a fuller understanding of the processes considered above.

Acknowledgements. This research was supported by the Swedish Natural Science Research Council (NFR), and by the Swedish Agency for Research Cooperation with Developing Countries (SAREC). Grants of computer time at the National Supercomputing Centre (NSC) in Linköping and the Centre for Parallel Computers (PDC) in Stockholm are gratefully acknowledged.

References

1. See, e.g. (a) Lund A, Lindgren M, Lunell S, Maruani J (1989) In: Maruani J (ed) Molecules in physics, chemistry, and biology, vol 3. Kluwer, Dordrecht, p 259; (b) Shida T, Egawa Y, Kubodera H, Kato T (1980) J Chem Phys 73:596
2. Merer AJ, Schoonveld L (1969) Can J Phys 47:1731; Köppel H, Domcke W, Cederbaum LS, von Niessen W (1978) J Chem Phys 69:4252
3. Lunell S, Huang MB (1990) Chem Phys Lett 168:63, and references therein; Eriksson LA, Malkin VG, Malkina OL, Salahub DR (1994) Int J Quantum Chem 52:879
4. (a) Shiotani M, Nagata Y, Sohma J (1984) J Am Chem Soc 106:4640; (b) Fujisawa J, Sato S, Shimokoshi K (1986) Chem Phys Lett 124:391
5. Alvarez-Idaboy JR, Eriksson LA, Fängström T, Lunell S (1993) J Phys Chem 97:12737
6. Jungwirth P, Bally T (1993) J Am Chem Soc 115:5783
7. Alvarez-Idaboy JR, Eriksson LA, Lunell S (1993) J Phys Chem 97:12742
8. (a) Toriyama K, Nunome K, Iwasaki M (1984) Chem Phys Lett 107:86; (b) Shiotani M, Nagata Y, Sohma J (1984) J Phys Chem 88:4078; (c) Clark T, Nelsen SF (1988) J Am Chem Soc 110:868;

(d) Lunell S, Eriksson LA, Huang MB (1991) J Mol Struct (Theochem) 230:263
9. Fujisawa J, Sato S, Shimokoshi K, Shida T (1985) J Phys Chem 89:5481
10. Pople JA, Nesbet RK (1954) J Chem Phys 22:571
11. Binkley JS, Pople JA, Hehre WJ (1980) J Am Chem Soc 102:939
12. (a) Møller C, Plesset MS (1934) Phys Rev 46:618; (b) Binkley JS, Pople JA (1975) Int J Quantum Chem 9:229; (c) Pople JA, Binkley JS, Seeger R (1976) Int J Quantum Chem Symp 10:1
13. See, e.g. Clark T (1985) A handbook of computational chemistry. Wiley, New York, Chap. 5
14. Hariharan PC, Pople JA (1973) Theor Chim Acta 28:213
15. Slater JC (1974) Quantum theory of molecules and solids, vol 4. McGraw-Hill, New York
16. Vosko SH, Wilk L, Nusair M (1980) Can J Phys 58:1200
17. The original three-parameter hybrid was suggested by Becke: Becke AD (1993) J Chem Phys 98:1372. A slightly modified form is implemented in the Gaussian programs: Stephens PJ, Devlin FJ, Chablowksi CF, Frisch MJ (1994) J Phys Chem 98:11623
18. Lee C, Yang W, Parr RG (1988) Phys Rev B 37:785
19. Boys SF, Bernardi F (1970) Mol Phys 19:553
20. See, e.g. Schwenke DW, Truhlar DG (1985) J Chem Phys 82:2418; Schwenke DW, Truhlar DG (1986) J Chem Phys 84:4113, and references therein
21. See, e.g. Frisch MJ, DelBene JE, Binkley JS, Schaefer III HF (1986) J Chem Phys 84:2279, and references therein
22. See, e.g. van Duijneveldt FB, van Duijneveldt-van de Rijdt JGCM, van Lenthe JH (1994) Chem Rev 94:1873, and references therein
23. GAUSSIAN 92, Revision C. Frisch MJ, Trucks GW, Head-Gordon M, Gill PMW, Wong MW, Foresman JB, Johnson BG, Schlegel HB, Robb MA, Replogle ES, Gomperts R, Andres JL, Raghavachari K, Binkley JS, Gonzalez C, Martin RL, Fox DJ, Defrees DJ, Baker J, Stewart JJP, Pople JA (1992) Gaussian, Inc., Pittsburgh, Pa
24. GAUSSIAN 94, Revision B2. Frisch MJ, Trucks GW, Schlegel HB, Gill PMW, Johnson BG, Robb MA, Cheeseman JR, Keith T, Petersson GA, Montgomery JA, Raghavachari K, Al-Laham MA, Zakrzewski VG, Ortiz JV, Foresman JB, Cioslowski J, Stefanov BB, Nanayakkara A, Challacombe M, Peng CY, Ayala PY, Chen W, Wong MW, Andres JL, Replogle ES, Gomperts R, Martin RL, Fox DJ, Binkley JS, Defrees DJ, Baker J, Stewart JJP, Head-Gordon M, Gonzalez C, Pople JA (1995) Gaussian, Inc., Pittsburgh, Pa
25. Meot-Ner M, Sieck LW, El-Shall MS, Daly MD (1995) J Am Chem Soc 117:7737
26. Dong XC, Salhi-Benachenhou N, Lunell S (1997) J Mol Struc (Theochem) 392:111
27. Stewart JJP (1990) QCPE program #581, Indiana University, Bloomington, Ind
28. Williams FF, Guo QX, Bebout DC, Carpenter K (1989) J Am Chem Soc 111:4133
29. (a) Andzelm J, Wimmer E (1992) J Chem Phys 96:1280; (b) Becke AD (1992) J Chem Phys 96:2155; (c) Johnson BG, Gill PMW, Pople JA (1993) J Chem Phys 98:5612; (d) Laming GJ, Termath V, Handy NC (1993) J Chem Phys 99:9765
30. Salhi-Benachenhou N, Alvarez-Idaboy JR, Lunell S (1997) Acta Chem Scand 51:242